

## MULTIPIION PRODUCTION IN DEUTERON-DEUTERON INTERACTIONS AT 7.9 GeV/c

A. T. Goshaw\*

Palmer Physical Laboratory, Princeton University, Princeton, New Jersey 08540

and

M. J. Bazin†

Physics Department, Rutgers University, New Brunswick, New Jersey 08903

(Received 11 March 1970)

Pion pair production is studied in the pure state of isospin  $T=0$  using the reaction  $dd \rightarrow dd\pi\pi$  in a bubble chamber experiment. The data are compared in detail with a one-pion-exchange and a Reggeized one-pion-exchange model including proper Bose symmetrization and the effects of the deuteron spin. No additional  $\pi\pi$  interaction is necessary to explain our data. A  $\pi\pi$  mass plot in bins close to our experimental resolution is presented as an incentive for bump hunters.

We have examined pion production in deuteron-deuteron collisions at a laboratory momentum of 7.9 GeV/c via the channels

$$dd \rightarrow dd\pi^+\pi^-, \quad (1)$$

$$\rightarrow dd\pi^+\pi^-\pi^0, \quad (2)$$

and

$$\rightarrow dpn\pi^+\pi^-. \quad (3)$$

Interest in Reactions (1) and (2) stems from the fact that, since the deuteron has isotopic spin zero, the  $\pi^+\pi^-$  or  $\pi^+\pi^-\pi^0$  system produced must be an isoscalar. In particular, Reaction (1) provides the possibility of studying the  $T=0$   $\pi\pi$  interaction without any  $T=1$  or 2 background. We present a detailed analysis of Reaction (1) which shows that at this energy a simple dynamical picture can predict the main features of the  $dd\pi^+\pi^-$  final state and that it is therefore likely that this production reaction is a rather insensitive probe of the  $T=0$   $\pi\pi$  interaction proper (at least at the statistical level of this experiment). Furthermore, although Reaction (3) imposes no selection rules on the  $\pi^+\pi^-$  system's isotopic spin, we find experimentally that its characteristics are similar to those of Reaction (1).

The experiment was carried out in the Brookhaven 80-in. bubble chamber filled with deuterium and exposed to an electrostatically separated beam of 7.90-GeV/c deuterons. A total of 75 000 pictures was taken representing a 2-event/ $\mu\text{b}$  exposure. The beam purity was monitored carefully since a small proton contamination could cause a serious background [e.g., the process  $pd \rightarrow pd\pi^+\pi^-$  is kinematically indistinguishable from Reaction (1) and has an appreciably larger cross section]. A Čerenkov counter (>99% efficient for protons) was used to record for each beam pulse whether any particle lighter

than a deuteron entered the bubble chamber. This indicated a beam purity greater than 97%. Of the pictures containing an identified  $dd$  interaction of interest, a fraction  $(20 \pm 4)\%$  was accompanied by a Čerenkov signal; with eight tracks per picture this is consistent with the 3% impurity recorded for the beam as a whole and indicates that there is no significant accumulation of proton-induced events in our sample. In addition, the deuterium used in the bubble chamber was analyzed and the free (molecularly bound) proton contamination found to be less than 0.9%; furthermore, events coming from such contamination would be suppressed by  $dd\pi^+\pi^-$  four-constraint kinematic fits because the target particle is required at the scanning stage to stop in the liquid. The above information allows us to say that at least 90% of our events are caused by a primary  $dd$  collision.

The events were selected by scanning for four-pronged interactions (thereby neglecting deuterons with momenta less than 130 MeV/c and protons with momenta less than 80 MeV/c). The preliminary selection of events insures that the beam deuteron does not break up by demanding that it scatter by less than  $4^\circ$  and lose less than 2 GeV/c in momentum. The slow deuteron was required to stop in the chamber within 30 cm of the vertex. These requirements force the four-momentum transfer to either deuteron to be less than  $\sim 0.3$  (GeV/c) $^2$ , which results in a negligible loss of events due to the sharp momentum-transfer dependence of the deuteron form factor. After application of these scanning selection criteria we were left with 10 000 events to measure.

All candidates were fitted using the standard THRESH-GRIND analysis programs. Reaction (1) is experimentally very well determined by a

Table I. Cross sections for pion production processes in  $dd$  collisions at 7.90 GeV/c.

Final state	Number of events	Cross section ( $\mu\text{b}$ )
$dd\pi^+\pi^-$	58	$27_{-5}^{+4}$
$dd\pi^+\pi^-\pi^0$	12	$<7$
$dd\eta$	$<2$	$<1.5$
$dd\omega$	0	$<1$
$dpn\pi^+\pi^-$	239	$330 \pm 30$

four-constraint fit. The main background, coming from Reaction (3), was evaluated by examining the distribution of  $\cos\theta_{pn}$  of the angle between the proton and the neutron in the laboratory for all events fitting Reaction (3). The  $dd \rightarrow dd\pi^+\pi^-$  contribution was then extracted by looking at the excess of events at  $\cos\theta_{pn} \geq 0.8$  [for Reaction (3) the  $\cos\theta_{pn}$  distribution is isotropic]. This procedure, and a weighted event assignment based on the  $\chi^2$  of the fit, gave consistent estimates which indicate a background of approximately 7 events in the sample used for the  $dd\pi^+\pi^-$  analysis.

The number of events observed in each channel is given in Table I along with the physical cross sections. An estimate of losses due to unseen slow protons and deuterons has been made. The background corrections to the  $dd\pi^+\pi^-$  final state are well defined as discussed above, but the few  $dd\pi^+\pi^-\pi^0$  events we observe may be contaminated by the  $dd \rightarrow dpn\pi^+\pi^-\pi^0$  ( $\pi^0$ ) reaction in a manner that is difficult to estimate. Therefore we can only put an upper limit of  $7 \mu\text{b}$  on Reaction (2). By examining the  $\pi^+\pi^-\pi^0$  mass distribution from all events fitting  $dd \rightarrow dd\pi^+\pi^-\pi^0$  we can put upper limits of  $1.5 \mu\text{b}$  on the production process  $dd \rightarrow dd\eta$  and  $1 \mu\text{b}$  on  $dd \rightarrow dd\omega$ . With regard to Reaction (3), only those events in which the fast (incident) deuteron did not break up were selected by our scanning procedure. This provided us with a subsample of events which could be fit well kinematically. One half of Reaction (3) was lost by this procedure. This and other experimental losses have been corrected for in estimating the cross sections given in Table I.

We now proceed with an analysis of the dynamics responsible for  $dd \rightarrow dd\pi^+\pi^-$ . First of all, it is important to recognize that there is a se-

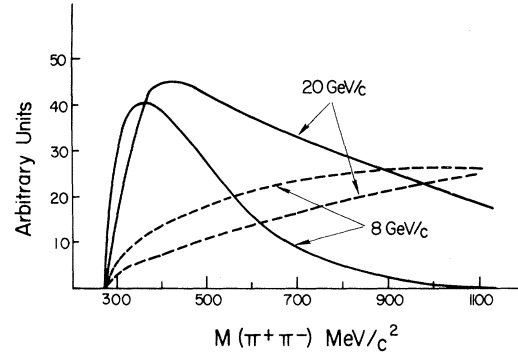


FIG. 1. Phase space (dashed curves) and form-factor-modified phase space (solid curves) for the  $\pi^+\pi^-$  mass distribution in the reaction  $dd \rightarrow dd\pi^+\pi^-$  at 7.9 and 20 GeV/c.

vere "kinematic" suppression of the  $ddX^0$  final state since the deuteron form factor is very strongly peaked at small momentum transfers:  $F_d(t) \propto e^{-34t}$  for  $t < 0.05$  ( $\text{GeV}/c$ )<sup>2</sup>. Therefore it is desirable to go to as high an incident deuteron momentum as possible in order to open up the phase space for this production process. This is illustrated in Fig. 1.

Only six events of the type  $dd \rightarrow dd\pi^+\pi^-$  were observed in previous work<sup>1</sup> done at 3 GeV/c and therefore no analysis could be made concerning the production mechanism. Figure 2(a) shows the pure  $T=0$   $\pi^+\pi^-$  mass distribution from our experiment which is peaked at threshold and falls smoothly to zero at  $m_{\pi\pi} \approx 700 \text{ MeV}/c^2$ . This is qualitatively what would be expected on the basis of the form-factor-modified phase space shown in Fig. 1. Figure 2(b) shows the  $d\pi$  mass spectrum. This is dominated by the "d\*" enhancement at 2200 MeV which has been seen in many previous experiments where a deuteron and pion were produced in the final state.

We have been able to explain quantitatively the features of the  $dd \rightarrow dd\pi^+\pi^-$  production process in terms of the dynamics implied by the diagram in Fig. 2(c). This one-pion-exchange process is the simplest nonresonant mechanism that can be written down for Reaction (1). The calculation has been done in some detail including explicitly the effects of Bose statistics, the deuteron spin, and the interference terms between exchange diagrams. The expression for the unpolarized differential cross section is

$$d\sigma = \frac{1}{(2\pi)^8 2^6 W_0 P_{c,m.}} \frac{1}{9} \sum_M |\mathfrak{M}^M|^2 \delta^4(P_{\text{final}} - P_{\text{initial}}) \frac{d^3\vec{P}_3 d^3\vec{P}_4 d^3\vec{P}_5 d^3\vec{P}_6}{P_{30} P_{40} P_{50} P_{60}}, \quad (4)$$

$$\mathfrak{M}^M = \mathfrak{M}_0^M + \mathfrak{M}_0^M (\pi^+ \text{ and } \pi^- \text{ interchanged}), \quad (5)$$

where

$$\mathfrak{N}_{\pi_0^M} = -i\mathfrak{N}_{\pi_d} m_1 m_3 (S_{35}, t_{13}, t_{35}^\pi) \mathcal{P}(t_{35}^\pi) \mathfrak{N}_{\pi_d} m_2 m_4 (S_{46}, t_{24}, t_{35}^\pi), \quad (6)$$

$$\mathfrak{N}_{\pi_d}^{mm'}(s, t, t_\pi) = 8\pi\sqrt{s} \sum_i f_i^{mm'}(s) P_i^{m-m'}(\cos\theta(s, t, t_\pi)). \quad (7)$$

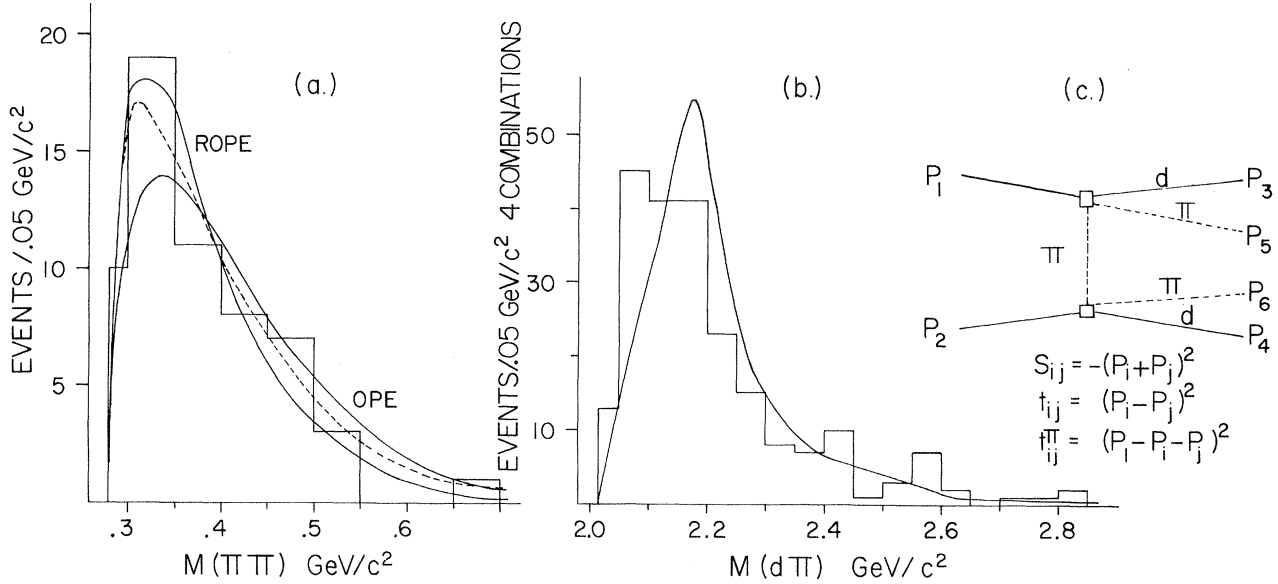


FIG. 2. (a) Experimental  $\pi\pi$  mass distribution in  $dd \rightarrow dd\pi^+\pi^-$ . The solid curves are normalized one-pion exchange (OPE) and Reggeized one-pion exchange (ROPE) predictions. The dashed curve is one-pion exchange with a pion-pion final-state interaction of scattering length  $1.5\hbar/m_\pi c$ . (b) Experimental  $d\pi$  mass distribution—the curve represents both OPE and ROPE predictions which are within 10% of each other. (c) Exchange diagram used for our theoretical predictions with definition of variables.

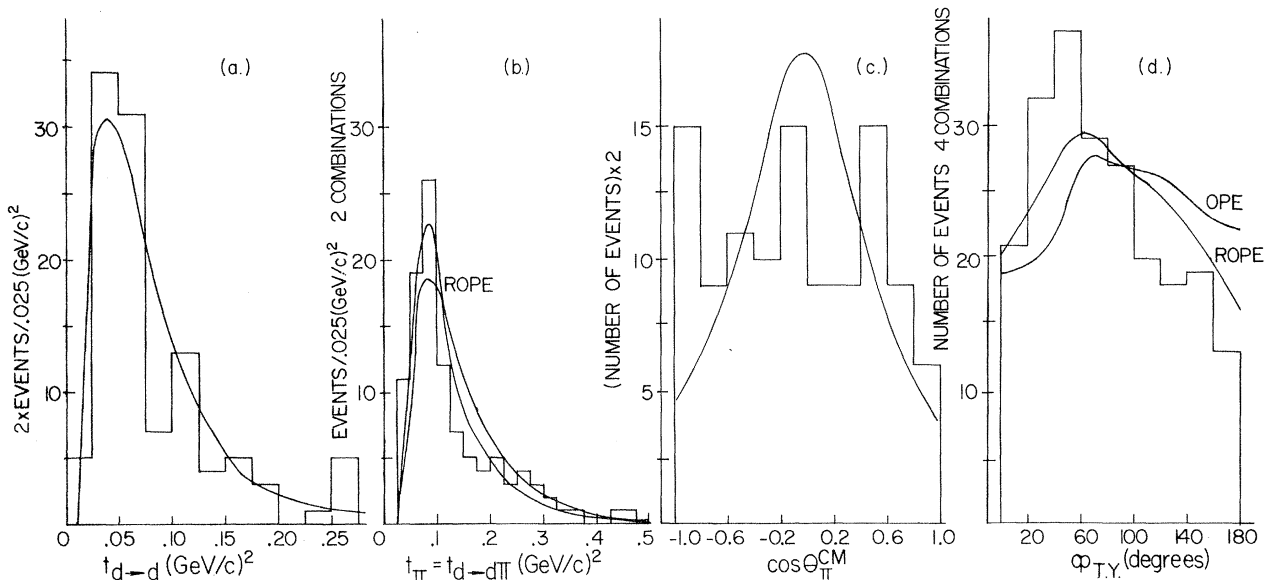


FIG. 3. (a) Distribution of squared momentum transfer for each deuteron (they are distinguishable experimentally). The curve is the theoretical prediction for which OPE and ROPE are indistinguishable. (b) Distribution of the squared momentum transfer of the virtual exchanged pion. The curves are the OPE and ROPE predictions. (c) Angular distribution of the pions in the production center-of-mass system. The curve is the theoretical prediction from OPE; the prediction from ROPE is within 10% of OPE. (d) Treiman-Yang angle distribution with theoretical OPE and ROPE predictions.

In these expressions,  $W_0$  is the total c.m. energy,  $P_{c.m.}$  is the c.m. momenta of the colliding deuterons, and the other kinematic variables are defined in Fig. 2(c). Equation (7) is the usual pole approximation for the virtual pion scattering at the upper or lower vertex.<sup>2</sup> The  $\pi d$  partial-wave amplitude  $f_l^{mm'}(s)$  was calculated using the impulse approximation and  $\pi N$  scattering amplitudes.<sup>3</sup> For the pion propagator  $\mathcal{O}$  both a single pole  $\mathcal{O}(t_\pi) = 1/(t_\pi - m_\pi^2)$  and a Reggeized trajectory of the form  $\mathcal{O}(t_\pi, S_{56}, t_{13}, t_{24}) = (\pi/\sqrt{2})(\cosh \xi_\pi/S_0) \times \alpha_\pi |1 - \cos \pi \alpha_\pi|^{-1/2}$ , with  $\alpha_\pi = (t_\pi - m_\pi^2)$ ,  $\cosh \xi_\pi = (S_{56} - t_{13} - t_{24}) - (m_\pi^2 - t_{13} - t_\pi)(m_\pi^2 - t_{24} - t_\pi)/2t_\pi$ , and  $S_0 = 1(\text{GeV})^2$  were tried. The Reggeized propagator systematically gave better agreement with the data although with differences negligible with respect to our experimental statistics. The calculations were done with Monte Carlo techniques including all experimental cuts, and the solid curves shown in Figs. 2 and 3 are the smoothed results.

We emphasize that the only input parameters are the pion-nucleon phase shifts and the deuteron wave function (taken from the Moravcsik III approximation<sup>4</sup>). The calculated total cross section is  $54 \mu\text{b}$  while the experimental one is  $25_{-5}^{+4} \mu\text{b}$  (both before correction for experimental cuts). Therefore the  $dd \rightarrow dd\pi^+\pi^-$  intensity is predicted to within a factor of 2, which is a reasonable success for this type of calculation. In the following we have normalized the various theoretical distributions to the number of observed events to best compare differential predictions.

The  $\pi^+\pi^-$  mass spectrum is satisfactorily explained with no  $\pi\pi$  or  $d\pi$  interactions other than those implied by Fig. 2(c). The Reggeized pion propagator gives a better fit than the simple one-pion exchange. However, if pion exchange is the basic mechanism for  $dd \rightarrow dd\pi^+\pi^-$  at this energy, then the  $\pi^+\pi^-$  mass spectrum can also be modified by introducing a  $T=0$   $\pi\pi$  interaction. This is illustrated by the dotted curve in Fig. 2(a) which is a OPE calculation including an S-wave  $\pi\pi$  interaction with the scattering length  $a_{00} = 1.5\hbar/m_\pi c$ . The Chew-Mandelstam effective-range formula was used for the  $\pi\pi$  interaction as done by Abashian, Booth, and Crowe.<sup>5</sup> Our data are not incompatible with a low-energy  $\pi\pi$ ,  $T=0$ , S-wave interaction of the Abashian-Booth-Crowe type with an effective range of order  $2\hbar/m_\pi c$ .

The  $d\pi$  mass spectrum shown in Fig. 2(b) presents the familiar  $d^*$  enhancement. This effect is not a resonance because the deuteron in each

$d\pi$  reference frame keeps its original direction of travel. We thus consider the enhancement as due to the large  $d\pi$  elastic cross section when the  $\pi N$  collision is near the  $N_{3,3}^*$  region.

Figure 3 shows some pertinent four-momentum and angular distributions and indicates where the bare (no absorptive corrections) calculations based on the graph of Fig. 2(c) break down. The four-momentum transfer to the deuterons is shown in Fig. 3(a). Its agreement with our calculation is based almost entirely on the deuteron form factor alone and lends support to treating the  $\pi d$  scattering via the impulse approximation. Figure 3(b) shows the four-momentum transfer across the virtual particle exchanged, which is sensitive to the propagator used in Eq. (6). The actual data have a somewhat sharper  $t$  dependence than predicted by simple OPE, and the Reggeized OPE model gives a slightly better fit. The pion angular distribution in Fig. 3(c) disagrees with theory ( $\chi^2$  probability is 2%). The Treiman-Yang angle distribution in Fig. 3(d) is compatible with the Reggeized model ( $\chi^2$  probability is 40%). Including a final-state  $\pi\pi$  interaction of any reasonable strength does not affect these angular distributions. The cause of the sharp anisotropy in the theoretical prediction for the angular distribution of the pions in the production center-of-mass system can be traced to the behavior of the  $\pi d$  scattering matrix element; it is not generated by either the form factors or the propagator. Thus the disagreement with the data undoubtedly reflects the presence of the  $\pi d$  final-state interaction between a  $\pi$  and a  $d$  from different vertices which are expected to be appreciable because of the large  $\pi d$  total cross section and the fact that all combinations of  $\pi d$  masses are experimentally concentrated near low masses.

Considering that  $\pi\pi$  interaction effects have

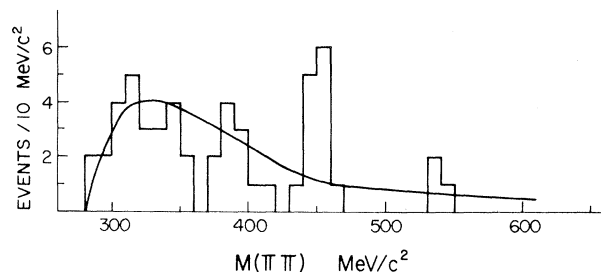


FIG. 4.  $\pi\pi$  mass distribution in 10-MeV/ $c^2$  bins. The curve is the ROPE prediction normalized to the full 54 events.

been reported in the low  $\pi\pi$  mass region several times in the past,<sup>6,7</sup> we present our  $\pi\pi$  mass spectrum in Fig. 4 in bins of  $10 \text{ MeV}/c^2$  since our experimental resolution is between 5 and  $10 \text{ MeV}/c^2$  for a  $\pi\pi$  mass near  $450 \text{ MeV}/c^2$ . The spike consisting of 11 events at  $M(\pi\pi) = 450 \text{ MeV}/c^2$  with a width less than  $10 \text{ MeV}/c^2$  is compatible with the resonance claimed by Goldzahl et al.<sup>7</sup> A similar plot for the breakup reaction  $\bar{d}\bar{d} \rightarrow \bar{d}p\pi^+\pi^-$  in which the  $\pi\pi$  system is not restricted to a  $T=0$  state does not show any enhancement at this mass value. Considering the low statistics available, however, we refrain from drawing any dramatic conclusion in this matter until we obtain more data from a forthcoming exposure at a higher incident momentum.

\*Work supported by the U. S. Atomic Energy Com-

mission under Contract No. AT(30-1)-2137. Present address: CERN, Geneva, Switzerland.

†Work supported by the National Science Foundation under Contract No. GP 11053.

<sup>1</sup>J. Debaisieux, F. Grard, J. Heughebaert, R. Servranckx, and R. Windmolders, Nucl. Phys. **70**, 603 (1965); G. Gidal, private communication.

<sup>2</sup>E. Ferrari and F. Selleri, Nuovo Cimento **24**, 453 (1962).

<sup>3</sup>L. D. Roper, R. M. Wright, and B. T. Feld, Phys. Rev. **138**, B190 (1965).

<sup>4</sup>M. J. Moravcsik, Nucl. Phys. **7**, 113 (1958).

<sup>5</sup>N. Booth and A. Abashian, Phys. Rev. **132**, 2318 (1963).

<sup>6</sup>L. Dubal and M. Ross, in Proceedings of a Conference on the  $\pi\pi$  and  $K\pi$  Interactions, Argonne National Laboratory, 14-16 May 1969 (unpublished).

<sup>7</sup>B. Maglič, in *Proceedings of the Lund International Conference on Elementary Particles*, edited by G. von Dardel (Berlingska Boktryckeriet, Lund, Sweden, 1970).

#### PRODUCTION OF THE $L$ MESON IN THE FINAL STATE $K^-p \rightarrow K^-\pi^+\pi^-p$ AT $4.6 \text{ GeV}/c^*$

M. Aguilar-Benitez, V. E. Barnes,<sup>†</sup> D. Bassano, S. U. Chung,<sup>‡</sup> R. L. Eisner, E. Flaminio, J. B. Kinson, R. B. Palmer, and N. P. Samios

Brookhaven National Laboratory, Upton, New York 11973

(Received 4 May 1970; revised manuscript received 8 June 1970)

Evidence is presented for production of the  $L$  meson ( $M = 1745 \pm 20 \text{ MeV}$  and  $\Gamma = 100 \pm 50 \text{ MeV}$ ) in the reaction  $K^-p \rightarrow K^-\pi^+\pi^-p$  at an incident momentum of  $4.6 \text{ GeV}/c$ . It decays mainly into  $K^-\pi^+\pi^-$ , of which  $(20 \pm 20)\%$  goes via the  $K(1420)\pi$  state. No significant evidence is found for  $K(890)\pi$ ,  $K\omega$ ,  $K\phi$ , or  $K\eta$  decay modes. We do not observe  $K\pi\pi$  threshold enhancements for arbitrary  $K\pi$  mass selections.

The first evidence for a strange meson with mass about  $1780 \text{ MeV}$ , called the  $L$  meson, decaying into the  $K\pi\pi$  final state was presented by the Aachen-Bonn-CERN-London (I.C.)-Vienna collaboration studying  $K^-p$  interactions at  $10 \text{ GeV}/c$ .<sup>1</sup> These authors observed the decay of the  $L$  meson into several modes, namely,  $K(890)\pi$ ,  $K(1420)\pi$ ,  $K\rho$ ,  $K\omega$ , and  $K\pi\pi$ . Subsequent to this, several experiments<sup>2</sup> have also reported observation of the  $L$  meson. Recently a Lawrence Radiation Laboratory (LRL) group<sup>3</sup> has reported evidence for a  $K\pi\pi$  structure at a mass similar to the  $L$  meson but with a much larger width than previously observed. The only decay mode observed in this experiment was  $K(1420)\pi$ . However, their observation of low mass enhancements in the  $K\pi\pi$  spectrum associated with any  $K\pi$  mass selection suggests that a large fraction of their effect may be kinematical in origin. In this Letter we report observation of a narrow  $L$  enhancement in the  $K\pi\pi$  final state produced in  $K^-p$  interactions at  $4.6 \text{ GeV}/c$ . We observe a

large non- $K(1420)\pi$  decay mode and do not observe low-mass  $K\pi\pi$  enhancements for arbitrary  $K\pi$  mass intervals. We therefore favor the resonance interpretation of the  $L$  enhancement.

The data for this analysis come from a 150 000-picture exposure of the Brookhaven National Laboratory (BNL) 80-in. hydrogen bubble chamber to a separated  $K^-$  beam of  $4.6\text{-GeV}/c$  momentum. The main reaction of interest for this study is

$$K^-p \rightarrow K^-\pi^+\pi^-p. \quad (1)$$

A total of 5415 events fit Reaction (1) (four-constraint hypothesis) with a  $\chi^2$  probability  $>1\%$  and measured ionization (from the BNL flying spot digitizer) consistent with the kinematic identification. This corresponds to a sensitivity of about 4 events/ $\mu\text{b}$ . In Fig. 1(a) we display the  $K^-\pi^+\pi^-$  effective-mass spectrum with the  $\Delta^{++}(1238)$  [defined as  $1.12 \leq M(p\pi^+) \leq 1.34 \text{ GeV}$ ] removed. A large  $Q$  enhancement ( $1200\text{-}1500 \text{ MeV}$ ) is clearly evident, as well as a significant effect in the  $L$  region. The solid curve represents the result